Available online at www.sciencedirect.com
SCIENCE DIRECT®
Journal of Molecular Catalysis A: Chemical 221 (2004) 127–136
JOURNAL OF MOLECULAR CATALYSIS A: CHEMICAL
www.elsevier.com/locate/molcata

Kinetics and mechanism of steady-state catalytic NO + O_2 reactions on Pt/SiO_2 and $Pt/CeZrO_2$

Rui Marques[a], Pierre Darcy[a], Patrick Da Costa[a], Henry Mellottée[a], Jean-Michel Trichard[b], Gérald Djéga-Mariadassou[a,*]

[a] *Laboratoire Réactivité de Surface, CNRS UMR 7609, Université Pierre et Marie Curie, Case 178, 4 Place Jussieu, 75252 Paris Cedex 05, France*
[b] *Renault SA, Technocentre Renault, 1 Avenue du Golf, 78280 Guyancourt, France*

Received 9 June 2004; accepted 23 June 2004
Available online 7 August 2004

Abstract

The kinetics of NO oxidation was performed over well-defined catalysts, Pt^0/SiO_2 and $Pt^{x+}/CeZrO_2$ being chosen as model zero-valent and oxidized platinum active sites, respectively. On both catalysts, the global rate equation was determined, leading to the partial orders in NO and O_2, and global rate constants. For both catalysts the orders in NO and O_2 are fractional and positive. Based on these data, two sequences of elementary steps are proposed. From the corresponding catalytic cycles, detailed kinetic rate laws were established leading to relevant kinetic constants and activation energies. Transient simulations were performed using the global power rate law and the detailed rate equations on both catalysts. A good fitting was observed up to 15% conversion on Pt^0/SiO_2, between 420 K and 500 K, with the global rate equation. The detailed kinetic data allowed a better fitting. For higher conversion the Arrhenius plots allowed us to conclude that diffusion limitations must be considered. A good fitting was observed over $Pt^{x+}/CeZrO_2$, between 420 K and 700 K, up to 25% conversion as expected with both global and detailed equations. Thermodynamic limitations are observed, in this case, above 30% conversion.

Keywords: NO oxidation; Pt^0/SiO_2; $Pt^{x+}/CeZrO_2$; Steady-state kinetics; Global and detailed rate equations; Rate constant; Catalytic cycles

1. Introduction

Automotive Diesel exhaust emission standards are more and more severe. In 2005, soot and NO_x productions will be limited to 25 mg km^{-1} and 250 mg km^{-1} respectively, according to Euro IV regulations, twice as low as for Euro III standards [1]. To meet those emission levels, car manufacturers have to use specific after-treatment systems: Diesel Particulate Filters for soot, NO_x-Trap and SCR for NO_x [2]. In these systems NO_2 has a key role, as it can be used as a strong oxidizer for de-soot processes [3] and as an intermediate for NO_x storage in NO_x-Traps [4] or for NO_x reduction in SCR [5]. However, in Diesel exhaust gas, NO is the major part of NO_x, thus it needs to be oxidized to NO_2 [6]. The oxidation of NO is then a very important reaction in Diesel exhaust conditions. It is therefore a bit surprising that kinetics of NO oxidation has not been extensively studied in the past. The attempt to model NO_x-Traps by Olsson et al. has led them to study the reaction over Pt/Al_2O_3 and $Pt/Ba/Al_2O_3$ [4,7,8]. They have proposed a mean field model, based on elementary steps. Parts of their kinetic parameters have been fitted to temperature programmed surface reaction (TPSR) results, and the others fixed to literature values [9]. However, no global kinetic parameters have been given. Instead, they have chosen an Eley–Rideal model in one of the papers [8]. Olsson et al. used a Langmuir–Hinshelwood (LH) model in their last paper on NO oxidation [9], as did Burch and Watling [5]. However, no clear experimental evidence has been given for either of these two models. It is important to remember that on a zero-valent Pt surface, NO dissociates when two platinum sites are adjacent [19]. On Pt^0, NO can adsorb undissociatively on a unique free site if this free site is enclosed by occupied sites [10]. Ollson's group results on

* Corresponding author. Tel.: +33 1 44 27 36 26; fax: +33 1 44 27 36 26.
E-mail address: djega@ccr.jussieu.fr (G. Djéga-Mariadassou).

1381-1169/$ – see front matter © 2004 Elsevier B.V. All rights reserved.
doi:10.1016/j.molcata.2004.06.023

Pt/Al_2O_3 have shown a decrease in Pt activity when the catalyst was exposed to NO + O_2 at 523 K [4]. This deactivation was attributed, according to XPS data, to the oxidation of Pt to PtO or PtO_2, which are less active than reduced platinum for NO oxidation. A decrease in activity has been also shown on Pt/SiO_2 by Xue et al. [11] and more recently by Desprès et al. [12]. Xue et al. attributed this to the build-up of some nitrogen and sulphur compounds on the active site of the platinum catalyst, and by the sintering of this catalyst. These authors have also observed a change in the TPR profile between fresh and deactivated catalysts, which could be linked to a change in the oxidation state of platinum. Desprès et al. have attributed the deactivation of Pt/SiO_2 to the formation of platinum oxide on the surface. The authors have also suggested an auto-inhibition of the NO oxidation reaction by NO_2. Moreover, NO oxidation has been considered as structure sensitive on Pt/Al_2O_3, the Pt activity decreasing for increasing Pt dispersion [4,13,14]. The reaction has also been found to be structure sensitive on Pt/SiO_2, while it seems structure insensitive on Pt/ZrO_2 [14]. The explanation has been linked to the deactivation of the catalyst, in the sense that small Pt particles more easily form oxides [4]. Another important feature of the NO oxidation is the thermodynamic equilibrium limitation, NO_2 decomposing to O_2 and NO at temperatures higher than 350 °C, depending on the oxygen partial pressure [6] and the presence of a catalyst.

In conclusion, the single reaction NO + 1/2 O_2 = NO_2 has not been investigated from the classical kinetic point of view, most papers determining kinetic parameters by fitting their experimental results with a NO_x-Trap model. Moreover, no global orders or global activation energies are available in the literature. Furthermore, let us note that the orders in respect to reactants, in global rate equation, have the potential to vary on the full range of conversion. A detailed rate equation based on a sequence of elementary steps can take into account the evolution of orders, insofar as thermodynamics does not limit the conversion. The purpose of this study is to investigate the NO oxidation over two different Pt catalysts. The first one is a reduced supported Pt^0 on SiO_2, while the second one is an oxidised cationic supported Pt^{x+} on CeO_2 (75%)–ZrO_2 (25%), referred to as $CeZrO_2$ in the text. The present work first determines the global kinetics and then more detailed rate laws, for the oxidation of NO over supported Pt^0 and Pt^{x+} catalysts. These kinetic data are then used to simulate the NO/O_2 TPSR carried out at the laboratory.

2. Experimental

2.1. Catalyst synthesis

The silica (Degussa, Aerosil 50) supported platinum (1.70 wt.% Pt) and the ceria-zirconia (25 wt.% CeO_2, Rhodia) supported platinum (0.35 wt.% Pt) catalysts were prepared by the incipient wetness method with an aqueous solution containing the appropriate amount of the platinum precursor H_2PtCl_6 (Alfa Aesar, purity 99.95%). After impregnation, the catalysts were dried at 393 K for 12 h. Before runs, the $CeZrO_2$ based catalysts were calcined at 773 K, for 2 h, in synthetic air (80% N_2, 20% O_2). The silica based catalysts were reduced in flowing hydrogen at 773 K, for 2 h, then flushed to He at room temperature (RT).

2.2. Dispersion measurements

Platinum catalysts, before and after reaction, were characterized by XRD, H_2–O_2 titration, and transmission electron microscopy (TEM). Elemental analysis was performed by the "Service Central d'Analyses du CNRS" in order to determine the platinum contents for both silica and ceria-zirconia supported catalysts. Powder X-ray diffraction (XRD) was carried out on a Siemens model D-500 diffractometer with Cu Kα radiation. High-resolution transmission electron microscopy (HRTEM) was performed to determine the size of platinum particles on silica and to check their dispersion. HRTEM studies were performed on a JEOL-JEM 100 CXII apparatus associated with a top entry device and operating at 100 kV. EDS analysis (STEM mode) was performed with the same apparatus using a LINK AN 10000 system, connected to a silicon-lithium diode detector, and multichannel analyser. EDS analyses were obtained on large domains of samples (150 nm × 200 nm to 400 nm × 533 nm).

The percentage of metal exposed (Pt% ME) was determined by hydrogen–oxygen titration using a conventional pulsed technique (Micromeretics). An insensitive structure reaction (benzene hydrogenation) was also used for counting $Pt^{(0)}$ species [15]. Measurements were conducted in a conventional device described elsewhere [16,17]. In a typical run, prior to benzene hydrogenation, catalysts were pretreated at 773 K in flowing hydrogen, then cooled to the reaction temperature under helium, and finally submitted to the H_2/C_6H_6 mixture. The number of exposed zero-valent Pt(0) atoms was deduced from the turnover rate of benzene hydrogenation [15].

2.3. Temperature programmed desorption of preadsorbed NO

Temperature programmed desorption (TPD) experiments of NO were carried out in flowing He (0.05 L min^{-1}) with a heating rate of 10 K min^{-1}, up to 723 K, after NO pretreatment. $Pt/CeZrO_2$ catalysts were calcined at 773 K for 2 h, and then cooled to room temperature. Pt/SiO_2 catalysts were reduced in H_2 at 773 K for 2 h with a heating rate of 10 K min^{-1}, the total flow rate being 0.20 L min^{-1}. The samples were then cooled to room temperature and hydrogen was switched to helium. Finally, Pt/SiO_2 catalysts were heated in He at 573 K to remove the hydrogen adsorbed on Pt/SiO_2 samples. Before TPD, $Pt/CeZrO_2$ and Pt/SiO_2 catalysts were finally flushed with He before gas mixture adsorption (770 ppm NO in He as balance, 0.20 L min^{-1}).

2.4. Steady-state NO + O_2 reaction rate measurements

NO, He, O_2 and a calibration gas mixture were used in NO + O_2 reaction kinetic measurements. NO was supplied by Air Liquide as 1.5 vol.% NO and 98.5 vol.% He (<10 ppm other gases). The oxygen, used for catalyst pretreatments and reaction kinetic measurements, was supplied by Alphagaz (UHP grade, <10 ppm other gases). Helium (UHP grade, Alphagaz) was used for dilution of the (NO + O_2) mixture to achieve lower NO and O_2 concentrations. Steady-state (NO + O_2) reaction rates were measured using a quartz microreactor (inner diameter 8 mm) containing quartz wool supporting the sample. The catalyst bed contained from 25 mg to 50 mg samples. All experiments were carried out at atmospheric pressure. The bed temperature was measured using a K-type thermocouple affixed to the outer reactor surface. The temperature was controlled using an electronic controller (Eurotherm 2408). Gas mixture were produced with calibrated electronic mass flow controllers (Brooks 5850TR). The reactor outflow was analyzed using a set of specific detectors. A Thermo Environmental Instruments 42CHL NO_x Chemiluminescence analyzer allowed the simultaneous detection of NO, NO_2 and NO_x (i.e. NO + NO_2). An Ultramat 6 Siemens IR analyzer was used to monitor N_2O. The signals of different gases were monitored on-line by Virtual Bench–Lab View computation programs.

NO oxidation transient experiments were modeled with the help of Microsoft Excel XP 2002 software using a personal computer on the basis of the kinetics (global and detailed) described in this work.

3. Results and discussion

3.1. Reduced or oxidized platinum species on the surface of catalysts

The purpose of this study deals with the oxidation of NO over platinum-based catalysts with various oxidation states of platinum. The first one is a silica-supported platinum catalyst, and the second a $CeZrO_2$ supported platinum catalyst.

Table 1 presents the platinum content and the percentage of metal exposed (PME) on both supported catalysts. Two different platinum loadings were used in order to synthesize a catalyst containing only zero-valent platinum (Pt^0/SiO_2) and a second one with only platinum with a higher oxidation state (Pt^{x+}/CeO_2–ZrO_2). The platinum contents were respectively 0.35 wt.% and 1.70 wt.% for $CeZrO_2$ and SiO_2. The Pt/SiO_2 catalyst exhibited a PME ranging from 19% to 21% depending on the titration process. Furthermore, 0 mol% of platinum was exposed as zero-valent metal atoms on $CeZrO_2$ taking into account the absence of benzene hydrogenation on this material. In the case of Rhodium, and according to the titration of Rh^{x+} by NO on a catalyst Rh(0.30 wt.%)/$CeZrO_2$ [18], the active sites consist of dispersed Rh^{x+} ions surrounded by two oxygen vacancies of the reduced support and associated with Ce^{3+} cations. In the case of Pt, it is considered that the active sites on Pt^{x+}(0.35 wt.%)/$CeZrO_2$ also consist of 100% platinum dispersed as Pt^{x+} ions (no Pt^0 active in benzene hydrogenation).

Table 1
Composition and platinum percentage of metal exposed (Pt% ME) of the synthesized catalysts

Catalysts	Pt (wt.%)	H_2–O_2	Pt% ME benzene hydrogenation (%)
Pt/SiO_2	1.70	21.3	19.5
$Pt/CeZrO_2$	0.35	–	0

As a consequence, the platinum was well dispersed on $CeZrO_2$, as confirmed by TEM and EDS, in which the Pt/Ce ratios are constant and close to those expected theoretically. In the case of Pt^0/SiO_2, the reduced metal was detected by XRD. Furthermore TEM showed platinum particles well dispersed on SiO_2, with an average particle size of 10 nm. In conclusion, two different platinum-based catalysts were synthesized, a supported zero-valent platinum catalyst, Pt^0/SiO_2, and a supported Pt^{x+} catalyst: $Pt^{x+}/CeZrO_2$.

3.2. Adsorption and subsequent desorption of NO on platinum catalysts

Adsorption of NO by flowing 1.5 vol.% NO in He, at room temperature, was carried out on platinum catalysts. During the adsorption on Pt^0/SiO_2, N_2O formation was observed (Fig. 2a). This result is in agreement with the literature and Burch et al. [10,19] have proposed that nitrogen monoxide dissociates on platinum reduced sites. At low temperatures, these authors have claimed that the most likely means of nitrogen atom removal involves the reaction between a nitrogen monoxide molecule adsorbed on a single isolated free site, *, and an adjacent adsorbed nitrogen atom, to yield N_2O [19] (Eq. (3)).

$$NO^{(1)} + 2^* \rightarrow {}^*N^{(1)} + {}^*O; \quad \sigma = 1 \tag{1}$$

$$NO^{(2)} + {}^* \rightarrow {}^*NO^{(2)}; \quad \sigma = 1 \tag{2}$$

$${}^*NO^{(2)} + {}^*N^{(1)} \rightarrow N_2O + 2^*; \quad \sigma = 1 \tag{3}$$

Global equation:

$$2NO = N_2O + {}^*O$$

Clearly, an oxygen atom is therefore left adsorbed on the surface during the dissociative adsorption of the first $NO^{(1)}$ molecule (Eq. (1)). Furthermore, these authors have clearly shown the competition, on reduced Pt^0 patches of the catalyst surface, between nitrogen monoxide adsorption/dissociation and the coverage of the Pt^0 sites by the dissociative adsorption of dioxygen.

On the contrary, on $CeZrO_2$ based catalysts, there is no release of N_2O during NO adsorption at RT.

TPD profiles of NO preadsorbed at RT over $CeZrO_2$ and $Pt/CeZrO_2$ are given in Fig. 2b.

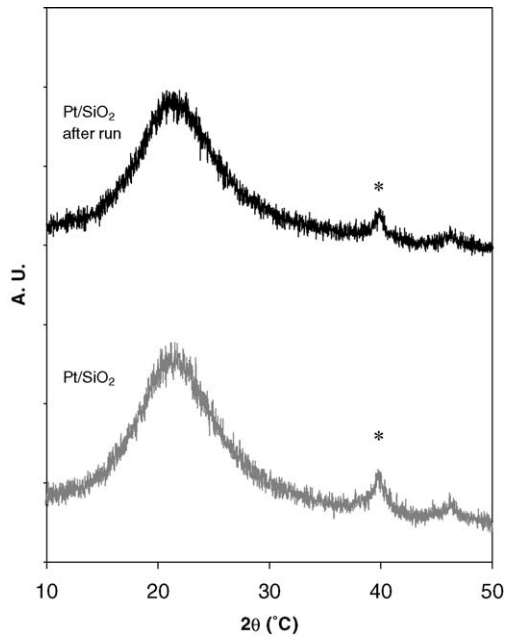

Fig. 1. X-ray diffraction patterns of Pt^0/SiO_2 (*: XRD lines of Pt^0).

On Pt^0/SiO_2, the NO release is not significant, which means that there are few isolated free sites on silica-supported platinum (1.7 wt.%) catalyst. On the contrary, two NO desorption peaks at 410 K and 480 K for $Pt^{x+}/CeZrO_2$, and 480 K and 570 K for $CeZrO_2$, are shown. On $Pt^{x+}/CeZrO_2$, the desorption peak at 410 K is attributed to the desorption of NO from either platinum or cerium cationic sites (Pt^{x+} or Ce^{x+}). Indeed, thermodynamic equilibrium indicates that NO_2 cannot decompose to NO at such a low temperature. These Pt^{x+} catalytic centers allow the molecular chemisorption of two adjacent NO molecules and the N–N bond formation, leading to N_2 [20]. This general scheme was already proposed by Djéga-Mariadassou et al. on $Rh^{x+}/CeZrO_2$ for the CO-assisted catalytic reduction of NO under three-way operating conditions [21]. The shift of the first desorption peak to lower temperatures (from 500 K ($CeZrO_2$) to 400 K ($Pt^{x+}/CeZrO_2$)) clearly illustrates the effect of platinum in its cationic form when supported over $CeZrO_2$.

3.3. Catalyst deactivation

No deactivation was observed in the steady-state NO oxidation on $Pt^{x+}/CeZrO_2$, probably due to the oxidation state of platinum species.

On the contrary, a slow deactivation compared to the NO/O_2 reaction rate was observed on silica-supported platinum(0) catalyst. Indeed, the NO conversion decreased from 50% to 26%. A steady-state conversion is only observed after 20 h of run. This deactivation has already been observed on Pt^0/SiO_2 catalysts [11,12,22]. Xue et al. [11] have also observed a change in the TPR profile of fresh and deactivated

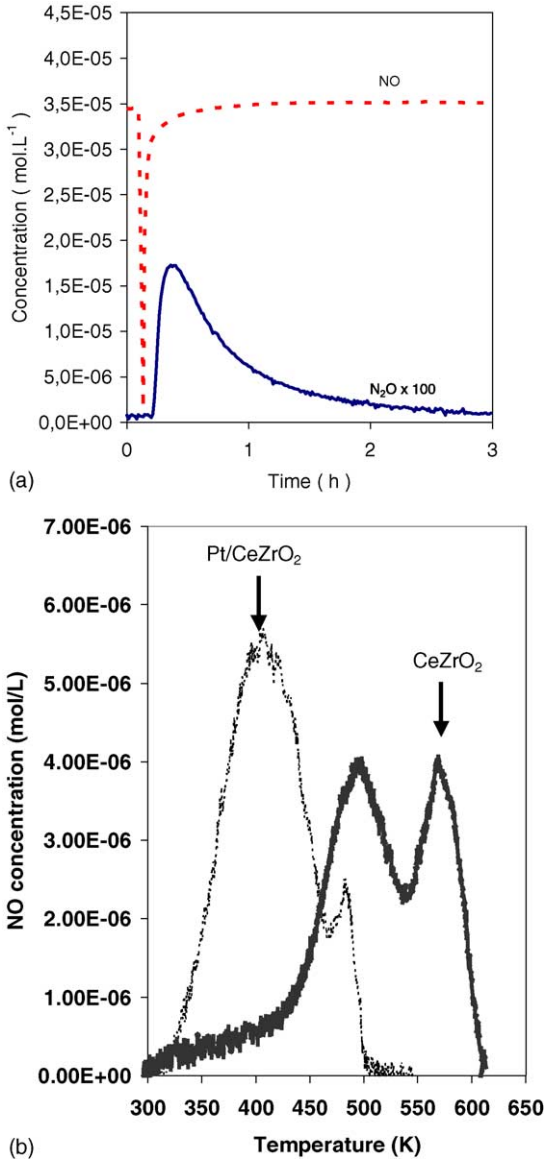

Fig. 2. (a) Adsorption, at room temperature, of 1.5 vol.% NO (0.05 L min^{-1}) in He on Pt/SiO_2 (50 mg); (b) temperature programmed desorption (TPD) in He (0.05 L min^{-1}) with a heating rate of 10 K min^{-1} on $CeZrO_2$, $Pt/CeZrO_2$.

catalysts, linked to a change in the oxidation state of platinum. Moreover, Burch et al. [19] proposed, on Pt-based catalysts, that the hydrocarbon reduces a patch of platinum atoms from "Pt–O" to platinum metal during a selective reduction of NO in Lean Burn conditions.

Our Pt^0/SiO_2 catalysts were characterized by TEM and XRD after runs. The XRD results are presented in Fig. 1. The average particle size of platinum remains around 10 nm. There is no sintering of platinum particles during the reaction. The observed deactivation can then be attributed to a strong Pt–oxygen interaction. This can lead to the formation of "Pt–O" species on the catalysts, as already observed in the literature on Pt-based catalysts [4,11,12,23,24]. However, the *bulk* Pt particles remained zero-valent platinum, as seen by

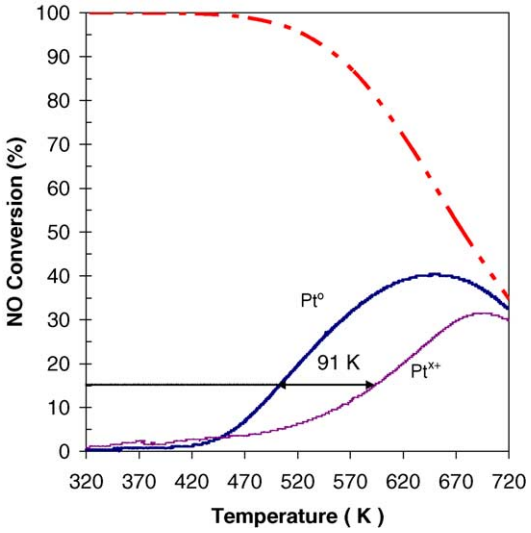

Fig. 3. NO conversion on $Pt/CeZrO_2$ (Pt^{x+}) and Pt/SiO_2 (Pt^0) (50 mg) during a temperature programmed surface reaction (TPSR) experiment in the following reaction conditions: 500 ppm NO, 9.6 vol.% O_2 in He as balance (total flow: 0.05 L min^{-1}) with a heating rate of 10 K min^{-1}; calculated thermodynamic plot for the same NO/O_2 mixture (—- - -—).

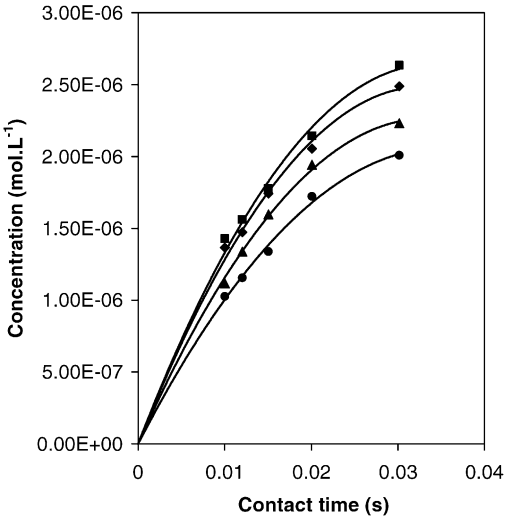

Fig. 4. NO_2 concentration vs. contact time for Pt^0/SiO_2 with 50 mg of catalyst, 7.7% O_2, (■) 1000 ppm NO, (♦) 700 ppm NO, (▲) 500 ppm NO, (●) 300 ppm NO.

XRD (Pt^0), Pt–O being an inhibited Pt species and representative of a very strongly linked oxygen species.

3.4. Kinetic study of the NO + O_2 reaction

3.4.1. Temperature reaction window and thermodynamic limitations (Fig. 3)

Let us note that both Pt^{x+} ($Pt/CeZrO_2$) and Pt^0 (Pt/SiO_2) present the same number of sites.

The thermodynamics of NO oxidation under 8 vol.% oxygen and 500 ppm NO is reported in Fig. 3. The NO conversion was calculated from Stull et al. data [25]. Moreover, NO conversions observed during the temperature programmed surface reaction are also reported for both Pt^{x+} ($Pt/CeZrO_2$) and Pt^0 (Pt/SiO_2). The temperature range for the kinetic study of the steady-state NO oxidation reaction was chosen to obtain less than 15% NO conversion. According to Fig. 3, a difference of 91 K was found between $Pt^{x+}/CeZrO_2$ and Pt^0/SiO_2. As a consequence, for the kinetic study, 15% NO conversion was taken into account, corresponding to 490 K and 581 K for Pt^0/SiO_2 and $Pt^{x+}/CeZrO_2$ respectively.

3.4.2. Kinetics of TPSR NO oxidation on Pt^0/SiO_2

3.4.2.1. Initial rate determination. According to the TPSR data, the temperature of NO oxidation reaction was chosen at 500 K in order to work at low NO conversion. After the initial deactivation, a quasi-steady state of the reaction was observed.

The initial rate r_{NO} (mol L^{-1} s^{-1}) was calculated from Fig. 4 at a constant O_2 concentration (7.7 vol.%), and various NO concentrations (ranging from 300 ppm to 1000 ppm). The initial rate r_{O_2} (mol L^{-1} s^{-1}) was also calculated fixing the NO concentration (equal to 500 ppm) and using various O_2 concentrations (ranging from 3.25 vol.% to 11.5 vol.%). In each case, NO conversions lower than 15% were used, and only data at low contact time were used ($t_c < 0.02$ s). Initial rates are reported, for each operating condition, in Table 2a.

The same calculations, for NO oxidation over $Pt^{x+}/CeZrO_2$ catalysts, are presented in Table 2b.

3.4.2.2. Orders in NO and O_2. The apparent orders in NO and O_2 were calculated from Ln–Ln plots with the initial rates from Table 2a. The orders are 0.30 and 0.44 in NO and O_2 respectively. The global activation energy was also calculated and found to be 57.7 kJ mol^{-1} (Table 3). The resulting experimental global power rate is:

$$r = k_{app}[NO]^{0.30}[O_2]^{0.44} \quad (4)$$

Table 2
Initial rates (mol l^{-1} s^{-1}) calculated for different operating conditions

NO (ppm)	O_2 (vol.%)	Initial Rate 10^4 (mol l^{-1} s^{-1})
(a) Pt^0/SiO_2		
300	7.7	1.02
500	7.7	1.11
700	7.7	1.36
1000	7.7	1.42
500	3.85	8.11
500	9.60	1.19
500	11.50	1.28
(b) $Pt^{x+}/CeZrO_2$		
300	7.7	5.98
500	7.7	8.55
1000	7.7	12.60
500	3.85	6.06
500	6.20	7.74
500	9.23	8.94

Table 3
Kinetic parameters associated to the NO–O_2 rate equation $r = k_0 \exp(-E_a/RT) P_{NO}{}^{\alpha} P_{O_2}{}^{\beta}$ over zero-valent and oxidized platinum species

Catalysts	Catalytic site	T (K)	α	β	E_a (kJ mol^{-1})	TOR[a] (10^{-4} s^{-1})
Pt/SiO_2	Pt^0	490	0.30	0.44	57.7	0.03
$Pt/CeZrO_2$	Pt^{x+}	581	0.62	0.47	34.6	0.08
$Pt/CeZrO_2$	Pt^{x+}	490				0.01

[a] Calculated with $[L] = 9 \times 10^{-7}$ mol Pt.

3.4.2.3. Sequence of elementary steps and detailed rate equation. The net reaction is $2NO + O_2 = 2NO_2$ and the global power rate equation (Eq. (4)) is:

$$r = k_{app}[NO]^{\alpha}[O_2]^{\beta} \quad (5)$$

With experimentally $\alpha = 0.30$ and $\beta = 0.44$.

In the literature, only Desprès et al. [12] proposed a sequence of elementary steps of the studied reaction. From global rate equations, we found that, on both catalysts, the mathematical orders in NO and O_2 are fractional and positive (Table 3). Consequently, a sequence of elementary steps and a detailed rate equation can be proposed.

According to Djéga-Mariadassou and Boudart [15], the symbols for elementary steps in a sequence are as follows: (→) far equilibrium step; σ, stoichiometric number according to the net reaction; (=), net equation.

Two catalytic routes can be considered on Pt^0/SiO_2. The first one involves an Eley–Rideal elementary step (Eq. (10)) and the second one, a Langmuir–Hinshelwood elementary step (Eq. (9)). Taking into account the strong concentration of oxygen atoms adsorbed on the surface ($^*O$), step 1 Eq. (6) and step 2 Eq. (7) mean that:

Step 1 Eq. (6): there is only one isolated free site accessible to form $^*O_2$. This last species is the point stage of dioxygen adsorption.
Step 2 Eq. (7): a free site is now adjacent to $^*O_2$. This second free site leads to the complete dissociation of preadsorbed dioxygen and the formation of an atomic adsorbed oxygen ($^*O$).

$$O_{2(g)} + {}^* \rightarrow {}^*O_2, \quad k_1; \quad \sigma_{LH} = 1, \quad \sigma_{ER} = 1 \quad (6)$$

$$^*O_2 + {}^* \rightarrow 2{}^*O, \quad k_2; \quad \sigma_{LH} = 1, \quad \sigma_{ER} = 1 \quad (7)$$

$$NO_{(g)} + {}^* \rightarrow {}^*NO, \quad k_3; \quad \sigma_{LH} = 2, \quad \sigma_{ER} = 0 \quad (8)$$

$$^*NO + {}^*O \rightarrow NO_{2(g)} + 2^*, \quad k_4; \quad \sigma_{LH} = 2, \quad \sigma_{ER} = 0 \quad (9)$$

$$NO(g) + {}^*O \rightarrow NO_{2(g)} + {}^*, \quad k_5; \quad \sigma_{LH} = 0, \quad \sigma_{ER} = 2 \quad (10)$$

$$2NO_{(g)} + O_2 = 2NO_{2(g)}; \quad \text{net equation} \quad (11)$$

Two sets of σ values are given leading the same net equation, but following either a LH step (σ_{LH}) or an ER one (σ_{ER}).

In this sequence, * stands for a Pt^0 free site, $^*O_2$ is defined as a molecular adsorbed oxygen on an initial *isolated* free active site. $^*O$ is an atomic oxygen adsorbed on an active site. $^*NO$ stands for a nitrogen monoxide adsorbed on an initial *isolated* active site. If all elementary steps are far equilibrium, there is no LH mechanism [15, pp. 92–101].

So let us consider first an ER step for the reaction (route corresponding to σ_{ER}). The detailed rate equation for this sequence is established following the method described by Djéga-Mariadassou and Boudart [15]. First, the application of the quasi–stationary state approximation (QSSA), considering Eqs. (6) and (10), leads to Eq. (12):

$$r\left(\frac{Pt^0}{SiO_2}\right) = \frac{r_5}{\sigma_5} = \frac{r_1}{\sigma_1} = \frac{k_5[NO][O^*]}{2} = k_1[O_2][^*] \quad (12)$$

Then, the balance on the density of sites is considered:

$$[L] = [^*] + [^*O] + \cdots \quad (13)$$

$^*O$ being the most abundant reaction intermediate (MARI),

From Eqs. (12) and (13):

$$[L] = [^*] + [O^*] = [^*]\left(1 + \frac{2k_1[O_2]}{k_5[NO]}\right) \quad (14)$$

Finally, the rate becomes:

$$r\left(\frac{Pt^0}{SiO_2}\right) = k_1[O_2][^*] = \frac{k_1 k_5[NO][O_2]}{2k_1[O_2] + k_5[NO]}[L] \quad (15)$$

For $0 < \alpha < 1$ and a domain where X is almost constant, one can write [15]:

$$X^{\alpha} = \frac{X}{1+X} \quad (16)$$

Then from Eq. (15), with $k'_5 = k_5/2$:

$$\begin{aligned}\frac{r(Pt^0/SiO_2)}{[L]} &= \frac{k_1[O_2]k'_5[NO]}{k'_5[NO]\left[1 + (k_1/k'_5)([O_2]/[NO])\right]} \\ &= \frac{k'_5[NO][k_1[O_2]/k'_5[NO]]}{1 + k_1/k'_5[O_2]/[NO]} \\ &= k'_5[NO]\left[\frac{k_1[O_2]}{k'_5[NO]}\right]^{\alpha} \\ &= [k'_5[NO]]^{1-\alpha} k_1{}^{\alpha}[O_2]^{\alpha}\end{aligned}$$

$$= [k_1{}^{\alpha} k'^{1-\alpha}_5][O_2]^{\alpha}[NO]^{1-\alpha}$$
$$= k_{exp}[O_2]^{\alpha}[NO]^{\beta} \quad (17)$$

In which, $1 - \alpha = \beta$· Mathematically, $\alpha + \beta = 1$. Experimentally, we found $r_{(Pt/SiO_2)} = k_{exp}[NO]^{0.30}[O_2]^{0.44}$ which leads to $\alpha + \beta \cong 0.8$, due to the standard deviation on the order calculations.

Let us note that Eq. (17) looks like but is not a generalized Langmuir–Hinshelwood equation as there is no equilibrium constant [15]. However, we cannot exclude that a LH *step* exists in the sequence of elementary steps. In that case, only steps 1 (Eq. (6)) to 4 (Eq. (9)) in the proposed sequence have to be considered. Let us note that if the adsorbed NO (*NO in step 4 (Eq. (9))) is rapidly consumed, that is, if k_4 is higher than k_3, steps 3 + 4 (Eqs. (8) and (9)) are equivalent to step 5 (Eq. (10)). So kinetic study does not able us to distinguish between a mechanism considering only an ER sequence elementary step or a LH elementary step.

3.4.3. Kinetics of transient NO oxidation on $Pt^{x+}/CeZrO_2$

The kinetics of ($NO + O_2$) reaction over oxidized platinum species has never been reported up to now by other groups. The same methodology already used for Pt^0/SiO_2 was used with $Pt^{x+}/CeZrO_2$.

3.4.3.1. Net reaction and overall rate equation. For NO conversion lower than 15%, initial rates of O_2 and NO consumptions were determined (Table 2b). The initial rate r_{NO} (mol L^{-1} s^{-1}) was calculated at a constant O_2 concentration, corresponding to 7.7 vol.%, and using various NO concentrations (from to 300 ppm to 1000 ppm). Similarly, the initial rate r_{O_2} (mol L^{-1} s^{-1}) was calculated at constant NO concentration (500 ppm) and using various O_2 concentrations (corresponding to 3.25 vol.% to 11.5 vol.%). The global partial orders in NO and O_2, respectively α and β in Eq. (5), are reported in Table 3. The global rate equation was found as follows:

$$r_{(Pt/CeZrO_2)} = k_{app,(Pt/CeZrO_2)}[NO]^{0.62}[O_2]^{0.47} \quad (18)$$

The global activation energy (Table 3) was found equal to 34.65 kJ mol^{-1}.

3.4.4. Sequence of elementary steps and detailed rate equation

The following sequence considers a platinum cation, stabilized at the surface of the ceria-zirconia support and surrounded by two oxygen vacancies. A unique complex active site, as already considered with other metals such as rhodium [16,19,21,22], is necessary for the reaction to turn over.

The unique site is denoted □ Pt^{x+}□ as for a complex in homogeneous catalysis [21]. The sequence of elementary steps is as follows:

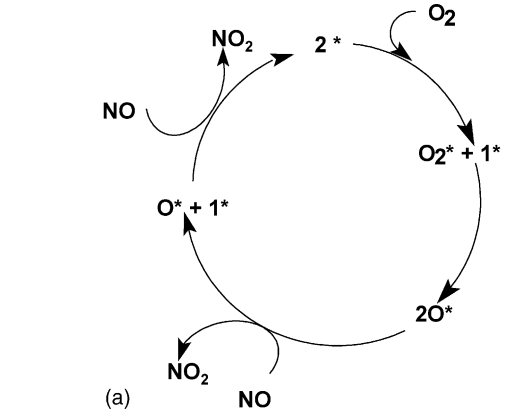

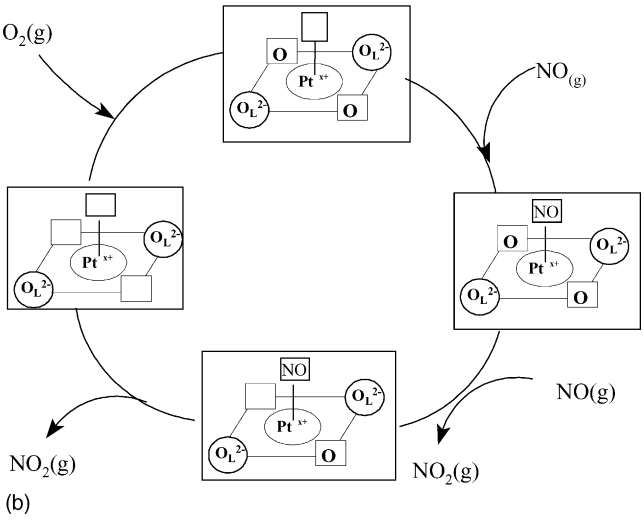

Fig. 5. Catalytic cycles for NO oxidation on (a) Pt^0/SiO_2 and (b) $Pt^{x+}/CeZrO_2$.

$$\square Pt^{x+}\square + O_{2(g)} \rightarrow OPt^{x+}O, \quad k_1; \quad \sigma = 1; \quad \square: \text{ vacancy} \quad (19)$$

$$OPt^{x+}O + NO_{(g)} \rightarrow OPt^{x+}O(NO), \quad k_2; \quad \sigma = 1 \quad (20)$$

$$OPt^{x+}O(NO) \rightarrow NO_{2(g)} + \square Pt^{x+}O, \quad k_3; \quad \sigma = 1 \quad (21)$$

$$\square Pt^{x+}O + NO_{(g)} \rightarrow NO_{2(g)} + \square Pt^{x+}\square, \quad k_4; \quad \sigma = 1 \quad (22)$$

$$2NO_{(g)} + O_{2(g)} = 2NO_{2(g)}; \quad \text{net equation} \quad (23)$$

This sequence is presented as a close sequence in Fig. 5b. The same methodology was used to establish the detailed rate equation.

$$r\left(\frac{Pt}{CeZrO_2}\right) = \frac{r_2}{\sigma_2} = \frac{r_1}{\sigma_1} \quad (24)$$

$$r\left(\frac{Pt}{CeZrO_2}\right) = k_2[OPt^{x+}O][NO] = k_1[\square Pt^{x+}\square][O_2] \quad (25)$$

"$OPt^{x+}O(NO)$" represents two oxygen anions and NO as ligands in the coordinative sphere of the platinum cation. "$\square Pt^{x+}O$" corresponds to one oxygen vacancy and one oxygen anion in the complex active site (the first oxygen anion has been consumed by reaction with the first NO molecule, see step 3 in the previous sequence).

If we consider that the MARI is "$OPt^{x+}O$" due the high affinity of ceria for oxygen, the balance on the density of sites becomes:

$$[L] = [OPt^{x+}O] + [\square Pt^{x+}\square] \quad (26)$$

Eqs. (25) and (26) lead to the detailed rate:

$$r\left(\frac{Pt}{CeZrO_2}\right) = \frac{k_1 k_2 [NO][O_2]}{k_1[O_2] + k_2[NO]}[L] \quad (27)$$

A similar detailed kinetic equation was reported on Rh^{x+}(0.29 wt.%)/$CeZrO_2$ for the CO + O_2 steady-state kinetic study [26].

3.4.5. Comparison of (NO + O_2) reaction kinetics over Pt^0/SiO_2 and $Pt^{x+}/CeZrO_2$ catalysts

The two catalytic cycles are reported in Fig. 5a and b for Pt^0/SiO_2 and $Pt^{x+}/CeZrO_2$ catalysts respectively. Both catalysts present fractional and positive apparent orders in NO and O_2. Kinetics leads to similar detailed rate equations,

$$r = \frac{k_{O_2} k_{NO}\,[NO]\,[O_2]}{k_{O_2}\,[O_2] + k_{NO}\,[NO]}[L] \quad (28)$$

However, the orders in respect to NO and O_2 are different.

In the detailed rate equations, Eqs. (15) and (27), k_{O2} stands for the rate constant of the adsorption of molecular oxygen on active sites, and k_{NO} stands for the rate constant of either the NO insertion on the active site ($Pt^{x+}/ZrCeO_2$) or the NO_{gas} reaction with the adsorbed oxygen on (Pt^0/SiO_2). Considering the linear transform (Eq. (29)) of Eq. (28),

$$\frac{1}{r} = \frac{1}{k_{NO}[NO][L]} + \frac{1}{k_{O_2}[O_2][L]} \quad (29)$$

kinetic measurements were performed with a fixed concentration of NO and various concentrations of O_2 as described therein, and also with a fixed concentration of O_2 and various concentrations of NO. By plotting $1/r$ versus $1/[O_2]$ at constant [NO] a linear regression was obtained. The values of the slope and the ordinate axis intercept allowed us to calculate k_{NO} and k_{O_2} over both supported Pt^0 and Pt^{x+} catalysts.

The same methodology, applied in a range of temperature from 465 K to 480 K on Pt^0/SiO_2 and from 565 K to 590 K on $Pt^{x+}/CeZrO_2$, led to the determination of the two corresponding activation energies and pre-exponential factors (Table 4a and b). The activation energies for the NO insertion and O_2 adsorption steps are 80.9 kJ mol^{-1} and 32.8 kJ mol^{-1} respectively, for Pt^0/SiO_2 (Table 4a), and 31.3 kJ mol^{-1} and 55.1 kJ mol^{-1} for $Pt^{x+}/CeZrO_2$ respectively (Table 4b). The two activation energies for the two considered steps are different. In the literature Ollson et al. [8,9] have found a similar activation energy, on Pt^0/Al_2O_3 catalysts, and for Pt^0/SiO_2, for the O_2 adsorption step (30.4 kJ mol^{-1}). However, they have proposed an activation energy for the NO insertion or adsorption close to those calculated on $Pt^{x+}/CeZrO_2$ (27.5 kJ mol^{-1}).

3.4.6. Simulation of the transient NO oxidation over Pt^0/SiO_2 and $Pt^{x+}/CeZrO_2$ catalysts

A perfect correlation is observed for both cases (Pt^0, Pt^{x+}) between the "detailed rate equation" simulated data and the experimental data up to 15% conversion, domain where the global kinetics was studied.

The kinetic parameters used in the simulation were optimized (values of the activation energies and the pre-exponential factor) to fit the experimental plot. The optimized values correspond to a maximum standard deviation of 5%, as it can be seen in Table 4a and b.

3.4.6.1. Simulation with global rate equations. The simulations of transient experiments over both catalysts are reported in Fig. 6a and b. The plots denoted 2 in Fig. 6a and b show the results using the experimental global rate equations corresponding to Eqs. (4) and (18) for Pt^0/SiO_2 and $Pt^{x+}/CeZrO_2$ respectively. For conversions lower than 15% corresponding to a domain controlled by kinetics, the calculated NO conversion versus temperature, and the experimental one (denoted 1 in Fig. 6a and b) fit very well for both catalysts. For higher conversions, the global rate law expressions simulated with Eqs. (4) and (18) for both catalysts, respectively, are no longer valid.

Table 4
Kinetic parameters associated to the NO–O_2 detailed rate equation

Catalysts	Catalytic site		A	E_a (kJ mol^{-1})	A cor[a]	E_a cor[a] (kJ mol^{-1})
Zero-valent species (a)						
Pt/SiO_2	Pt^0	O_2 adsorption	5.81×10^4	33.9	5.81×10^4	32.8
		NO insertion	2.27×10^{12}	85.2	2.50×10^{12}	80.9
Oxidized platinum species (b)						
$Pt/CeZrO_2$	Pt^{x+}	O_2 adsorption	6.45×10^6	58.0	6.45×10^6	55.1
		NO insertion	1.48×10^6	29.5	1.48×10^6	31.3

Experimental and corrected pre-exponential factors (A) and activation energy (E_a) of the oxygen adsorption and NO insertion of the reduced and the oxidized platinum sequence.

[a] Optimized values estimated considering a maximum standard deviation of 5% used for simulation.

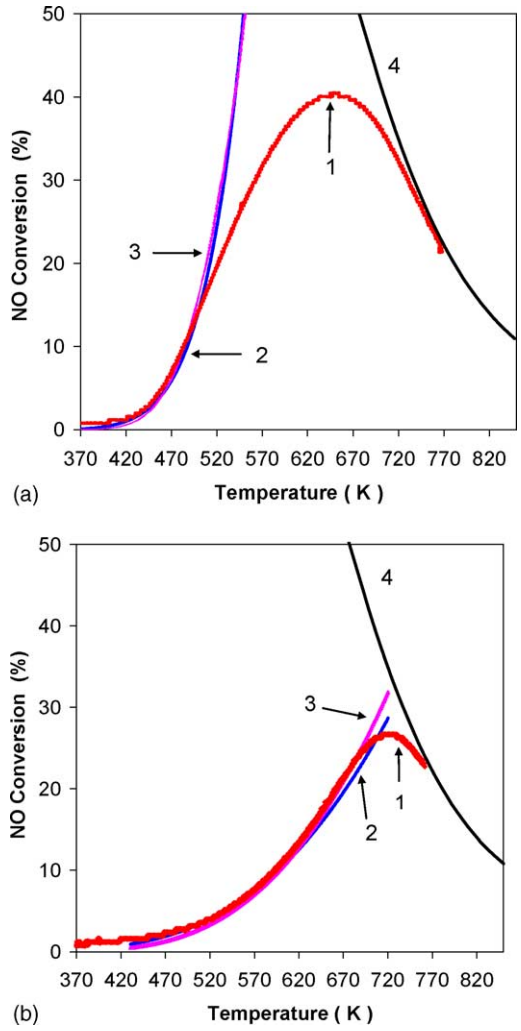

Fig. 6. Experimental (denoted 1) and simulated (denoted 2 and 3) temperature transient NO–O_2 data (3 K min^{-1}, 300–1000 ppm NO, 3.25–11.5 vol.% O_2 in He) over: (a) Pt^0/SiO_2, (b) $Pt^{x+}/CeZrO_2$, using for (2) the global power rate and for (3) a detailed rate kinetic equation, (4) Thermodynamic data.

3.4.6.2. Simulation with detailed rate equations. The simulations were also performed using the detailed rate equations Eqs. (15) and (27) for Pt^0/SiO_2 and $Pt^{x+}/CeZrO_2$ respectively; they are denoted 3 in Fig. 6a and b. It must be noted that the correlation between experimental and simulated data is better than that performed from the global rate equation.

3.4.7. Simulation limitations

For $Pt^{x+}/CeZrO_2$ catalysts, both global and detailed rate equation simulations fit well up to 25% of conversion, which is the maximum allowed by thermodynamics as reported in Fig. 3. On the contrary, for the NO + O_2 transient reaction on Pt^0/SiO_2, it seems that the thermodynamics is not a limit. For this catalyst, only a very good correlation between experimental and simulated data is obtained for a conversion lower than 20%.

Considering the Arrhenius plot of transient NO + O_2 reaction in a large domain of conversion on Pt/SiO_2, two domains were found (Fig. 7). The first one, at low conversion (low temperature) corresponds to a domain controlled by the kinetics; the activation energy found is nearly the same as given in Table 3. The second one, at a higher conversion, is controlled by diffusion. Indeed, the Arrhenius plot gives a slope corresponding to $-E_a/2RT$ which is significant of an internal diffusion [15]. Then, the limits of kinetic approach could be due to diffusion problems.

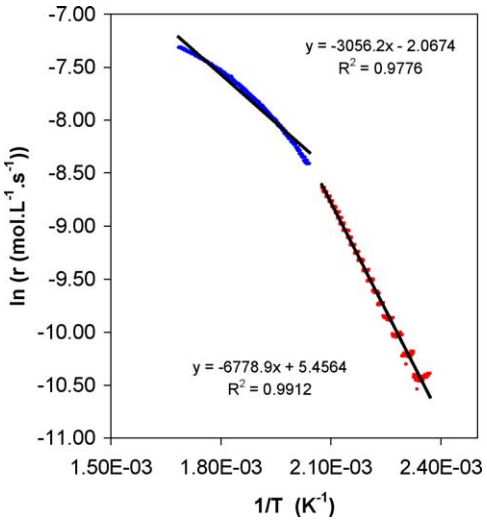

Fig. 7. Arrhenius plot for the k_{app} obtained from the regression for Pt^0/SiO_2, using the NO_2 conversion.

3.4.8. Catalytic activity

The turnover rates are also reported in Table 3. In fact, the reaction temperature is 91 K lower for Pt^0/SiO_2 to obtain 15% conversion. The TOR calculated for $Pt^{x+}/CeZrO_2$, at 490 K, is lower than those obtained for Pt^0/SiO_2. The values obtained for Pt^0/SiO_2 (0.03 s^{-1}) are in the same order of magnitude then those calculated by Xue et al. [14] (0.01 s^{-1}) on a similar catalyst Pt (2 wt.%)/SiO_2. Nevertheless, no TOR data were reported in the literature for this Pt^0/SiO_2. Only alumina or zirconia supported platinum catalysts were reported with TOR ranging from 0.005 s^{-1} to 0.03 s^{-1} [14].

4. Conclusion

Steady-state kinetics of NO + O_2 reaction was performed over supported platinum catalysts in two different oxidation states: Pt^0 for Pt/SiO_2 catalyst and Pt^{x+} for $Pt/CeZrO_2$ catalyst.

The Pt^0/SiO_2 catalyst exhibits a PME around 20%. On the contrary, 0 mol% of platinum was exposed as zero-valent metal atoms on $CeZrO_2$. According to the literature [19], with the titration of Pt^{x+} by NO, we can consider that the active sites are 100% exposed Pt^{x+} ions on $Pt/CeZrO_2$.

The global rate equations were determined at 500 K and 591 K for Pt^0/SiO_2 and $Pt^{x+}/CeZrO_2$, respectively. On both catalysts, the apparent orders in NO and O_2 were found frac-

tional and positive: $r_{(Pt/SiO_2)} = k_{app,(Pt/SiO_2)}[NO]^{0.30}[O_2]^{0.44}$ and $r_{(Pt/CeZrO_2)} = k_{app,(Pt/CeZrO_2)}[NO]^{0.62}[O_2]^{0.47}$. Detailed rate equations were established from sequences of elementary steps. For both catalysts, a similar rate expression was found: $r = (k_{O_2}k_{NO}[NO][O_2]/k_{O_2}[O_2] + k_{NO}[NO])[L]$. From this equation the corresponding rate constants (k_{NO}, k_{O_2}) and activation energies of elementary steps were calculated. Finally, simulations were performed using global and detailed rate expressions. On both catalysts, it was shown that global rate equations allowed for a satisfying fit of the transient NO + O_2 reaction up to 15% conversion, the range of experimental runs. For higher conversion, a strong deviation occurs over Pt^0/SiO_2 between simulated and experimental data, suggesting that the global rate equation is no longer valid. The simulations based on detailed rate equations allowed for a better fit of experimental. However, for conversion higher than 15% the same deviation was observed mainly over Pt^0/SiO_2. On $Pt^{x+}/CeZrO_2$, the limits of kinetics are clearly due to thermodynamic limitations. On the contrary, on Pt^0/SiO_2, internal diffusion was predominant.

Acknowledgements

This program was performed with the financial support of Renault S.A. P. Beaunier is greatly acknowledged for TEM experiments. The catalyst support ($CeZrO_2$) was purchased by Rhodia.

References

[1] A.A.L. Barry, M.M. Van Setten, J.A. Moulijn, Catal. Rev. (2001) 43.
[2] T.V. Johnson, SAE Technical Paper Series SAE 2002-01-0285, 2002.
[3] G. Mul, W. Zhu, F. Kapteijn, J.A. Moulijn, Appl. Catal. B (1998) 17.
[4] L. Olsson, E. Fridell, J. Catal. 210 (2002) 340.
[5] R. Burch, T.C. Watling, Stud. Surf. Sci. Catal. 116 (1998) 199.
[6] W.A. Majewski, J.L. Ambs, K. Bickel, SAE Technical Paper Series SAE 950374, 1995.
[7] L. Olsson, E. Fridell, M. Skoglundh, B. Andersson, Catal. Today (2002) 73.
[8] L. Olsson, B. Westerberg, H. Persson, E. Fridell, M. Skoglundh, B. Andersson, J. Phys. Chem. B 103 (1999) 10433.
[9] L. Olsson, H. Persson, E. Fridell, M. Skoglundh, B. Andersson, J. Phys. Chem. B 105 (2001) 6895.
[10] R. Burch, J.P. Breen, F.C. Meunier, Appl. Catal. B 39 (2002) 283.
[11] E. Xue, K. Seshan, J.G. Van Ommen, J.R.H. Ross, Appl. Catal. B 2 (1993) 183.
[12] J. Desprès, M. Elsener, M. Koebel, O. Kröcher, B. Schnyder, A. Wokaun, Appl. Catal. B 50 (2004) 73.
[13] J.H. Lee, H. Harold, Kung, Catal. Lett. 51 (1998) 1.
[14] E. Xue, K. Seshan, J.R. Ross, Appl. Catal. B 11 (1996) 65.
[15] M. Boudart, G. Djéga-Mariadassou, Kinetics of Heterogeneous Catalytic Reactions, Princeton University Press, Princeton, NJ, 1984.
[16] F. Fajardie, J.-F. Tempère, G. Djéga-Mariadassou, G. Blanchard, J. Catal. 163 (1996) 77.
[17] L. Salin, C. Potvin, M. Boudart, G. Djéga-Mariadassou, J.M. Bart, Ind. Eng. Res. 37 (1998) 4531.
[18] F. Fajardie, J.-F. Tempère, J.-M. Manoli, O. Touret, G. Blanchard, G. Djéga-Mariadassou, J. Catal. 179 (1998) 469.
[19] R. Burch, P.J. Millington, A.P. Walker, Appl. Catal. B 4 (1994) 65.
[20] O. Gorce, H. Jurado, C. Thomas, G. Djéga-Mariadassou, A. Khacef, J.M. Cormier, J.M. Pouvesle, G. Blanchard, S. Calvo, Y. Lendresse, SAE Paper 2001-01-3508, 2001.
[21] G. Djéga-Mariadassou, F. Fajardie, J.-F. Tempère, J.-M. Manoli, O. Touret, G. Blanchard, J. Mol. Catal. A 161 (2000) 179.
[22] J. Despres, M. Koebel, M. Elsener, A. Wokaun, PSI Scientific Report 2001, 2002, V64–V65.
[23] C.P. Hwang, C.T. Yeh, J. Mol. Catal. A 112 (1996) 295.
[24] C.B. Wang, C.T. Yeh, J. Catal. 178 (1998) 450.
[25] D.R. Stull, J.E.F. Westrum, et al., The Chemical Thermodynamics of Organic Compounds, Krieger, Malabar, FL, USA, 1987, pp. 201–233.
[26] I. Manuel, J. Chaubet, C. Thomas, H. Colas, N. Matthess, G. Djéga-Mariadassou, J. Catal. 224 (2004) 269.